HHS Public Access

Author manuscript

IEEE Trans Biomed Eng. Author manuscript; available in PMC 2015 December 09.

Published in final edited form as:

IEEE Trans Biomed Eng. 2014 April ; 61(4): 1062–1070. doi:10.1109/TBME.2013.2293779.

A Novel Reduced-Order Prioritized Optimization Method for Radiation Therapy Treatment Planning

Georgios Kalantzis and

Department of Medical Physics Memorial Sloan Kettering Cancer Center NYC, New York, NY 10065, USA

Aditya Apte

Department of Medical Physics Memorial Sloan Kettering Cancer Center NYC, New York, NY 10065, USA

Georgios Kalantzis: gkalan@gmail.com; Aditya Apte: adapte@mskcc.org

Abstract

In this study, a novel reduced order prioritized algorithm is presented for optimization in radiation therapy treatment planning. The proposed method consists of three stages. In the first stage, the intensity space was sampled by solving a series of unconstrained optimization problems. The objective function of the first stage is expressed as a scalarized weighted sum of partial objectives for the target and organ at risk. Latin hypercube sampling was utilized to define the weights for each run of the unconstrained optimizations. In the second stage, principal component analysis is applied to the solutions determined in the first stage to identify the major eigen modes in the intensities space, significantly reducing the number of independent variables. In the third stage, treatment planning goals/objectives are prioritized, and the problem is solved in the reduced order space. After each objective is optimized, that objective function is converted into a constraint for the lower-priority objectives. In the current formulation, a slip factor is used to relax the hard constraints for planning target volume (PTV) coverage. The applicability of the proposed method is demonstrated for one prostate and one lung intensity-modulated radiation therapy treatment plan. Upon completion of the sequential prioritized optimization, the mean dose at the rectum and bladder was reduced by 21.3% and 22.4%, respectively. Additionally, we investigated the effect of the slip factor ‘s’ on PTV coverage and we found minimal degradation of the tumor dose (~4%). Finally, the speed up factors upon the dimensionality reduction were as high as 49.9 without compromising the quality of the results.

Index Terms

Intensity modulated radiation therapy (IMRT); multiobjective optimization (MOO); prioritized optimization (PO)

Correspondence to: Georgios Kalantzis, gkalan@gmail.com.

Color versions of one or more of the figures in this paper are available online at http://ieeexplore.ieee.org.

I. Introduction

INTENSITY-modulated radiation therapy (IMRT) is an advanced mode of high-precision external radiotherapy that uses computer-controlled, mega-voltage x-ray accelerators to deliver precise doses of radiation to specific tissues. Rather than being treated with a large uniform beam, in IMRT, the patient is treated by a series of beam shapes that are modeled as a collection of pencil beams (beamlets). For many types of cancer, such as prostate cancer, the use of IMRT allows a highly concentrated treatment of the tumor volume, while limiting the radiation dose to adjacent healthy tissue [1]. IMRT treatment planning is concerned with selecting a beam geometry and beamlet intensities (fluence map) to produce the best dose distribution that can be delivered efficiently.

The concept of multiobjective optimization (MOO) for radiotherapy treatment planning has been an active area of research. IMRT uses inverse planning optimization to determine complex radiation beam configurations that will distribute the radiation dose to the patient [2]–[4]. The problem is inherently multiobjective, with competing clinical goals to deliver a high dose to the planning target volume (PTV) while minimizing the dose to organs at risk (OARs). These conflicting clinical objectives often require compromises when selecting a clinical treatment plan for a patient.

A number of increasingly sophisticated mathematical programming models have been proposed for inverse treatment planning (see [5] for a recent overview). One of the most common approaches to MOO is to optimize a single-objective function constructed from the weighted sum of multiple objectives, in which the weights denote different relative importance to different objectives [6], [7]. This is called the priori approach because the user is expected to provide the weights. The popularity of this method lies in its straightforward implementation and computational efficiency. In the past, gradient-based algorithms have been proposed for the optimization of single-objective problems in radiation therapy. However, the main disadvantage of these algorithms is that planner intervention is often required to conduct a multiple trial-error process, in which several parameters are varied until an acceptable compromise is achieved. One way to ameliorate that issue is to use the prioritized or lexicographic optimization method [8], [9]. Prioritized optimization (PO) is a form of multicriteria optimization, in which the various objectives under consideration cannot be quantitatively traded off between each other, at least not in a numerically tractable way. Instead, PO considers a finite number of objective functions that are to be optimized on a feasible set of solutions in a qualitatively prioritized order (i.e., lower-priority objectives are optimized as far as they do not interfere with the optimization of higher-priority objectives). The main advantage of that method is that it generates an optimal solution at every sequential stage and also, does not rely on interaction with the user once the prioritization is fixed. It should be noted that PO may be viewed as the limit of the minimization of a weighted combination of objectives, in which the weights are equal to different powers of a small parameter called “epsilon,” according to Danskin’s theorem [10]. However, numerical minimization of such a composite objective function with different orders of magnitude can lead to poorly conditioned problems. Therefore, the choice of weighting factors of the scalarized multicriteria objective function is a sensitive problem in itself.

For IMRT problems with planning goals that exhibit distinctive levels of importance or priority, previous studies have demonstrated that PO may provide an intuitive way of generating a solution [11]–[13]. However, PO has been criticized for not allowing a large gain on a low-priority goal in trading off a small loss on a high-priority goal [14]. Wilkens *et al*. [12] addressed that issue by introducing a slip factor, which allows small degradations of higher-priority goals to the benefit of lower-priority goals. In other words, the achievements of the algorithm for higher-priority objectives were relaxed by a certain amount, offering more flexibility in the algorithm for lower-order priorities. Additionally, constraint optimization for a large-scale problem, such as that in radiation therapy with several hundreds of variables (beamlet intensities), might become computationally intensive. In the past, dimensionality reduction techniques have proven to be a solution for decreasing the complexity and time of constraint optimization of the PTV for several anatomical sites [15]–[18] as well as generation of pareto frontiers with memetic algorithms [19]. The reduced-order Constraint optimization (ROCO) method offers a key advantage in that it involves a computational efficient constrained optimization step in which hard constraints are directly imposed on the optimization structures by reducing the dimensionality of the intensity space. The main drawback of ROCO is that the final constraint optimization in the reduced dimensionality search space is performed only on a single-objective quadratic function for the PTV.

This paper presents the first report, to the best of our knowledge, of a method of reduced-order PO for IMRT. In the next section, we describe our method in further detail and include a mathematical description of each step of the optimization. Section 3 shows the results with a prostate and a lung case, the effect of varying the slip parameter, and the number of principal components (p.c.) used during the dimensionality reduction procedure. We further discuss these results and some key issues in the final section of the paper.

II. Multiobjective Optimization for IMRT

A. Description of the Problem

An IMRT treatment plan has to specify a fluence map (a set of beamlet intensities that can be controlled individually). Typically, a small number of equispaced coplanar beam angles are used. The planned structures are modeled as discretized cubes (called voxels) and the dose to each voxel per intensity of each beamlet is calculated [20], [21]. A radiation oncologist specifies a set of requirements that have to be satisfied in the treatment plan. These requirements are in the form of the prescription dose to the PTV and the maximum dose at the OARs.

B. Hierarchical Optimization in Reduced Space

Hierarchical optimization is a strategy of multivariable optimization derived from priority-driven sequential steps of single-objective optimization problems. Without loss of generality, we consider the minimization of a multiobjective problem. Suppose a complex goal $g = \{g_1, g_2, \ldots, g_n\}$ contains n objectives. The subscript in this goal also describes the relative importance of each objective, where g_1 is the most important one and g_{i-1} is always more important than g_i. The solution $g^{(1)}=\{g_1^{(1)}, g_2^{(1)}, \ldots, g_n^{(1)}\}$ is better than the solution

$g^{(2)}=\{g_1^{(2)}, g_2^{(2)}, \ldots, g_n^{(2)}\}$, if, and only if, $g_k^{(1)}<g_k^{(2)}$ and $g_i^{(1)}=g_i^{(2)}=\min(g_i)$ hold for certain $k \leq n$ and all $i < k$. In other words, before priority k, all objectives are equally satisfied in both $g^{(1)}$ and $g^{(2)}$, but on priority k, $g^{(1)}$ dominates $g^{(2)}$. Thus, the formulation of the prioritized minimization problem can be written as follows:

$$\min g_k, k=1, 2, \ldots, n$$

$$\text{s.t.} g_i=\min g_i, i<k. \quad (1)$$

Accordingly, PO would be defined as the algorithmic process of a prioritized minimum solution for a multiobjective problem. In the current study, we employed a prioritized approach combined with a dimensionality reduction of the search space in order to reduce the computational complexity of the numerical optimization method for solving the sequential constrained optimization problems. An outline of our method can be written in generic form, as in Fig. 1.

Initially using a computed tomography scan as a guide, the number and orientation of beams to be used in the treatment were selected by the planner. Afterwards, a series of unconstrained optimizations were performed to sample the optimal intensity space. Upon completion of the unconstrained optimizations, a principal component analysis (PCA) was employed in order to reduce the dimensionality reduction of the solution space. Finally, sequential PO steps were performed with constraints in the reduced-order space. In the following subsections, we describe each stage of our method.

C. Sampling the Unconstrained Optimal Intensity Space

The inverse radiotherapy problem is to determine a vector of beamlet intensities that minimizes the objective function. In the first step of our method, our goal is to “probe” the intensity space for a given patient. To that end, we initially constructed a single-objective function expressed as a weighted sum of partial terms:

$$I=\arg \min w_T \sum_{i \in T} \frac{(D_i - D_T)^2}{N_T} + \sum_{j \in \text{OARs}} w_j \cdot <D_j> \quad (2a)$$

$$\sum_k w_k=1 \quad (2b)$$

where N_T is the number of voxels in the target structure, D_T is the prescribed dose to the PTV, $< D_j >$ is the mean dose of the OAR j, and the variables w_T and w_j are the relative weights for the PTV and OARs, respectively. The Latin hypercube sampling method was employed to define the weights variables of (1) in the interval [0, 1]. The dose to voxel i is given by:

$$D_i = \sum_{k=1}^{M} \sum_{j=1}^{N} A_{k,j} \cdot I_{k,j} \quad (3)$$

where A_k is the dose deposition matrix (DDM), which describes the dose contribution to all relevant voxels of the structure under consideration for the unit fluence; k is the index of the beam number; $I_{k,j}$ is the intensity of the beamlet j for the beam k;M is the total number of beams; and N is the number of beamlets for beam k. Parameter-based unconstrained optimization was used to construct an intensity space that contains possible solutions. We then applied PCA to reduce the dimensionality of the search space and make the constrained optimization computationally feasible.

D. Reduction of Search-Space Dimensionality

Upon sampling optimal intensities $\{I_1, I_2, \ldots, I_N\}$ (see (2)), the dimensionality of the intensity space can be reduced by linear or nonlinear feature extraction methods. PCA constructs a low-dimensional representation of the data (in our case, the intensities of the beamlets), which describes as much of the variance in the data as possible. This is accomplished by finding a linear basis of reduced dimensionality for the beamlet intensities, in which the amount of variance is maximal. It can be shown that this linear mapping is formed by the d-principal eigenvectors (i.e., p.c.) of the covariance matrix of the zeromean data. The corresponding eigenvectors form the columns of linear transformation matrix T. Low-dimensional data representations y of datapoints x are computed, mapping them onto linear basis T, i.e., $Y = (X - X_{\text{mean}}).T$. In our case, the dose of structure S in the reduced dimensionality space is given by:

$$D^S(\xi, N_{\text{modes}}) = \sum_{j=1}^{N_{\text{modes}}} A \cdot \xi_j + \mu \quad (4)$$

where ξ_j are the coefficients of the p.c., which are the independent variables of the optimization. Similarly, as A is the DDM previously, j is the index of the N_{modes} p.c., and μ is the dose corresponding to the mean of $\{I_i\}$. The intensities of these modes were determined during the PCA and the linear transformation is simply:

$$\xi_i = L^T I_i, I_i = L\xi_i + <\{I_i\}> \quad (5)$$

where L is a vector containing the eigenvectors and ξ_j are essentially the coordinates of the transformed intensities $\{I_i\}$. Given the p.c. variances (that is, the eigenvalues of the covariance matrix), we find the Λ eigenvectors that capture a desired percentage (v%) of the total variance:

$$v\% = \frac{\sum_{i=1}^{\Lambda} \lambda_i}{\sum_{j=1}^{M} \lambda_j} \geq 98\%. \quad (6)$$

E. Reduced-Order Prioritized Optimization

The mathematical formulation of the PO is similar to the one proposed by Wilkens *et al*. [12] and can be described as follows:

Step 1: Find the vector y in the eigenspace so as to:

$$\text{minimize}\mathrm{OF}^1(y)=\frac{\sum_{j\in T}[D_j(y)-D_{\text{presc}}]^2}{V_T} \quad (7a)$$

$$\text{s.t.:}D_j(y)\le D_{\text{OAR1}}^{\max},\forall_j\in V_{\text{OAR1}} \quad (7b)$$

$$L\cdot y+\langle\{I_i\}\rangle\ge 0 \quad (7c)$$

where $D_j(y)$ is the dose voxel j of the target T and is given from (4), and y is the beamlet intensities in the eigenspace; D_{presc} is the prescription dose; V_T and V_{OAR1} is the volume of the target and the OAR1, respectively; and $D_{\text{OAR1}}^{\max}$ is the constraint for the maximum dose at the OAR[1]. Equation (7c) requires the inversely transformed data y from the eigenspace to the real intensity values to be positive numbers.

Step 2: In the second step, we minimize the mean dose at the first OAR:

$$\text{minimize}\mathrm{OF}^2(y)=\frac{\sum_{j\in\text{OAR1}}D_j(y)}{V_{\text{OAR1}}} \quad (8a)$$

$$\text{s.t.:}D_j(y)\le D_{\text{OAR1}}^{\max},\forall_j\in V_{\text{OAR1}} \quad (8b)$$

$$\min[D_j(y^1)]\le D_j(y)\le D_j^{\max}\le\max[D_j(y^1),1.15\cdot D_{\text{presc}}],\ \forall_j\in T \quad (8c)$$

$$\mathrm{OF}^1(y)\le(1+s)\cdot\mathrm{OF}^1(y^1) \quad (8d)$$

$$L\cdot y+\langle\{I_i\}\rangle\ge 0 \quad (8e)$$

where $D_{\text{OAR1}}^{\max}$ and V_{OAR1} are the maximum dose allowed at and the volume of the OAR[1], respectively, and y^1 is the solution obtained in *Step 1*. We observe that we have two additional constraints for the optimization problem. First, the dose at the target should be greater than or equal to the minimum dose and greater than the maximum dose or 115% of the prescription dose, as they were obtained from *Step 1* (8c). Second, the hard constraint for the quadratic function OF^1 that was achieved in *Step 1* is relaxed by slip factors (8d). Similarly as in the previous step, we require the beamlets intensities to be positive numbers (8e).

Step 3: As before, *Step 3* reads as follows: Find y in order to:

$$\text{minimize}\mathrm{OF}^3(y)=\frac{\sum_{j\in \mathrm{OAR2}} D_j(y)}{V_{\mathrm{OAR2}}} \quad (9a)$$

$$\text{s.t.:}D_j(y) \leq D_{\mathrm{OAR1}}^{\max} \forall_j \in V_{\mathrm{OAR1}} \quad (9b)$$

$$D_j(y) \leq D_{\mathrm{OAR2}}^{\max} \forall_j \in V_{\mathrm{OAR2}} \quad (9c)$$

$$\min[D_j(y^1)] \leq D_j(y) \leq D_j^{\max} \leq \max[D_j(y^1), 1.15 \cdot D_{\mathrm{presc}}], \forall_j \in T \quad (9c)$$

$$\mathrm{OF}^1(y) \leq (1+s)^2 \cdot \mathrm{OF}^1(y^1) \quad (9d)$$

$$\mathrm{OF}^2(y) \leq \mathrm{OF}^2(y^2) \quad (9e)$$

$$L \cdot y + \langle \{I_i\} \rangle \geq 0. \quad (9f)$$

The hard constraints in *Step 3* are similar to those in *Step 2*, with the exception of (9e), which requests that the mean dose at the OAR^1 not exceed the mean dose for the same OAR that was obtained in *Step 2*. Additionally, the relaxation of constraints in OF^1 is increased by the square of (1+s).

F. Treatment Planning Optimization Parameters

In this paper, two treatment plans were used to evaluate our method. The first one was a prostate case with two OARs: the rectum and the bladder. The plan consisted of five coplanar beams (nominal energy, 6 MV) and a total number of 235 beamlets each of which were 1.0 cm^2 in size. The prescription dose to the PTV was 72 Gy, and the maximum dose at the bladder and the rectum was 105% of the prescribed dose. The second treatment plan was a lung case, with the lung and the heart considered OARs. The PTV was irradiated with three coplanar beams (nominal energy, 6 MV), and the number of beamlets was 272. For each case, we used 100 samples during the unconstrained optimization stage. For the numerical solver, the SQP algorithm was used [22], while the maximum number of iterations was set to 200 and the code was implemented in MATLAB (The MathWorks, Inc., Natick, MA, USA). Finally, the treatment planning was performed using the software environment CERR (Computational Environment for Radiotherapy Research) [23], and the DDM was calculated with the ORART (Operations Research Applied to Radiation Therapy) toolbox, which is an extension of CERR that is based on Ahnesjo's pencil beam algorithm [21], [24]. For all beams, the DDM was precalculated and stored in memory as a sparse matrix.

III. Results for a Prostate Case

A. Number of Samples and Eigenvalues

A critical aspect of our method is the choice of the number of p.c.. A small number of p.c. will not reliably capture the major modes of the intensity space. The screen plot in Fig. 2 (a) and (b) illustrates for the prostate and lung case, respectively, the eigenvalues and the percentage of variance explained for the first fifty p.c. From our data, we found that 42 p.c. were sufficient to capture 98% of the total variance for the prostate case, whereas it was 24 p.c. for the lung plan. Those p.c. were the independent variables of the PO procedure.

B. Prostate IMRT Case

For qualitatively demonstration of our method's results, we employed as a metric the dose-volume histograms (DVHs) which is commonly used in radiation therapy for evaluation of a treatment plan. The DVHs for the prostate IMRT case are shown in Fig. 3 for each structure and step separately. The *x*-axis represents the dose at the structure while the *y*-axis represents the fractional volume which have received a dose *D*. A slip factor s equal to 2 was used in this example. The goals of each individual step of the sequential optimization method are reflected by the DVHs. In *Step 1*, good coverage of the PTV is achieved, while the dose at the rectum and bladder do not exceed the maximum allowed dose. In *Step 2*, the dose at the rectum is substantially reduced and the homogeneity of the PTV is not affected significantly, but the mean dose to the bladder is slightly increased. Finally, in *Step 3*, the mean dose of the bladder is considerably decreased without compromising the mean dose at the rectum. For demonstration purposes, Fig. 4 illustrates traversal and sagittal views of the dose distributions for each step. The overlapping of the rectum and the bladder with the PTV was 6% and 17%, respectively. By visual inspection, one can notice dose sparing at the rectum in *Step 2* [see Fig. 4 (b) and (e)].

Table I reports the numerical results of our simulations. We should stress that the reported results were not normalized to deliver the prescription dose to the ICRU-50 [25] prescription point (isocenter). Such normalization would simply linearly escalate the dose of each structure for each step, so we therefore considered that the difference in the dose at each step would be more profound without normalization. In Table I, one can notice that the reduction of the PTV coverage (D_{95}~Dose received the 95% of the PTV volume) is equal to ~2%, while the mean dose at the rectum and the bladder was decreased by ~17% and ~18%, respectively, upon completion of the final step of the optimization, when a slip factor (s = 2) was used.

C. Lung IMRT Case

A lung IMRT case with a prescription dose to the PTV of 60 Gy was considered. Fig. 5 (a) illustrates the three steps of the PO. As before, two OARs were considered: the lung and the heart. Figs. 5 (b), (c), and (d) shows the DVHs for the PTV, lung, and heart, respectively, when a slip factor of 3 was used.

Fig. 6 shows the sagittal and traversal dose distributions of the treatment plan for each optimization step. As in the prostate case, we note the sparing of the lung and the heart during the second and third step, respectively, of the optimization.

In Table II, we see that the D_{95} was reduced by ~2%, while the mean dose at the lung and the heart were reduced by ~16% and ~55%, respectively. We speculate that the main reason for the dramatic decrease in the mean dose at the heart is that there is no actual overlap of this structure with the PTV. Therefore, the optimizer can more easily reduce the dose at the heart, without affecting the dose coverage of the PTV.

D. Effect of Slip Factor "s" and Eigenmodes

We carried out a set of simulations to investigate the effect of the slip factor s and the dimensionality reduction on our method.

A set of POs was repeated without dimensionality reduction of the intensity space and compared with the results obtained from our method. Table III reports the speed up factors obtained with our method compared to the nonreduced order POs for the two treatment planning cases. An average speedup of 36.3 and 43.5 was achieved for the prostate and lung case respectively. It is worth noting that a higher speedup factor was achieved for the lung case. That was expected since the number of eigen modes used for that plan (24 eigen modes) was smaller compared to the prostate case (42 eigen modes). That implies less independent variables and consequently smaller execution times.

Evaluation of the effect of the dimensionality reduction on the plans quality was based on the DVHs as this is the most common way in clinical practice. As can be seen in Fig. 7, there is a good agreement between our method and the nonreduced algorithm for both the prostate and lung case. Finally, Fig. 8 (a) and (b) illustrates for the prostate and lung case, respectively,

We observe that the maximum reduction of the D_{95} was ~4%, whereas the mean dose at the rectum and bladder was reduced by ~23%, compared to the maximum mean value. Similarly, for the lung case, the D_{95} was decreased by ~2% when a slip factor of 3 was used.

IV. Conclusion

We have described a reduced-order hierarchical programming method for IMRT treatment planning. The applicability of our method was demonstrated for a prostate and lung treatment planning case. The advantages of the proposed method over the 'conventional' approach of creating a linearly weighted multiterm objective function are: (i) qualitatively, priorities of objectives can be defined intuitively by the planner/physician before treatment planning optimization; (ii) once the hierarchy of the objectives and slip factor are determined, the process is automatic and does not require several trial and error optimizations. In that way, the planner can focus on the final evaluation of the treatment plan; (iii) since normal tissue dosimetric goals are used as objective functions, rather than simple constraints, the method reduces the dose to normal tissue as much as possible without

adversely affecting more important goals; and (iv) the reduction of the search-space dimensionality enhances computational efficiency of the sequential constraint optimizations.

In the current formulation, mean dose objective functions were used for the OARs for both the unconstrained sampling stage and the PO, in a manner similar to Wilkens *et al*. [12]. However, in clinical practice, dose-volume constraints are commonly used in addition to mean-dose constraints. Previous studies have incorporated dose-volume constraints in gradient-based algorithms for inverse treatment planning [26]. One disadvantage of dose-volume constraints is that they introduce nonconvex feasibility spaces into the optimization problem, potentially creating multiple local minima and associated issues in solver accuracy and run-time efficiency [27]. Thus, mixed-integer or heuristic techniques are required, and these are generally not as efficient as linear/quadratic methods. Additionally, for nonconvex regions, the weighted-sum approach cannot discover optimal solutions of the Pareto front [28], and one cannot assert that linear PCA will always detect all structures in a given data set [29]. In that case, nonlinear feature-extraction algorithms would be more adequate for the reduction of search-space dimensionality and abstraction of the structures in the beamlet intensities. Alternatively, Romeijn *et al*. have previously suggested using ‘mean tail dose’ rather than conventional dose-volume constraints [30], which are linear functions and hence, computationally attractive. ‘Mean tail dose’ refers to the mean dose of either the hottest or coldest specified fractional volume and has been successfully used in PO studies in the past [13]. However, one disadvantage of the ‘mean tail dose’ approach is the increase in problem size, which would result in extensive execution times.

A key variable of the current technique is the slip factor ‘s’. As previous studies have shown, a small relaxation of a higher-priority objective can result in a large improvement of a lower-priority goal [12], [13]. The studies indicated that, in the reduced-order space, the slip factor could significantly improve the average dose at the OARs, without significantly compromising the dose homogeneity at the PTV. Additionally, from our results it appears that reduction of the search-space dimensionality produces similar solutions with those obtained from the PO without utilizing dimensionality reduction.

We would like to stress that in the current study, we focus on the methodological aspects of the proposed algorithm, rather than investigate its performance under various conditions. Therefore, in our implementation, we did not extensively alleviate computational bottlenecks of the executable code, which might hinder its computational complexity and consequently, its performance. Despite the fact the code was implemented in MATLAB, which is slower when compared to other commercial software for constraint optimization, we observed a maximum acceleration of ~49.9 for PO. That is due to the decrease in independent variables of the numerical optimizer. The main disadvantage of our method, however, is the sampling stage, during which several optimization runs are required. GPU-based IMRT optimization [31] and parallel global optimizers [32], which result in significantly reduced execution times, have been suggested in the past. Future directions of our study involve parallelization of the numerical optimizer, which would lead to further acceleration of the proposed method.

Overall, the proposed reduced order prioritized-prescription treatment planning bears not only the ability to impact the dose distribution in a direct intuitive way, but also the enhanced computational efficiency makes the method attractive for clinical use.

Acknowledgment

The authors would like to acknowledge Dr. A. Jackson for his helpful comments.

This work was supported in part by the National Cancer Institute (NCI) under Grant 1R01CA148876-04. Its contents are solely the responsibility of the authors and do not necessarily represent the official views of the National Cancer Institute, National Institutes of Health.

References

1. Veldeman L, Madani I, Hulstaert F, Meerleer G, Mareel M, De Neve W. Evidence behind use of intensity-modulated radiotherapy: A systematic review of comparative clinical studies. Lancet Oncology. 2008:367–375. [PubMed: 18374290]
2. Bortfeld T. Optimized planning using physical objectives and constraints. Semin. Radiation Oncology. 1999; 9:20–34.
3. Fuks, Z.; Leibel, SA.; Ling, CC. A Practical Guide to Intensity-Modulated Radiation Therapy. Madison, WI, USA: Medical Physics Publishing; 2004.
4. Palta, R.; Mackie, TR. Intensity Modulated Radiation Therapy: The State of the Art. Madison, WI, USA: Medical Physics Publishing; 2004.
5. Kufer, K.; Monz, M.; Scherrer, A.; Suss, P.; Alonso, F.; Sultan, A.; Bortfeld, T.; Thieke, C. Multicriteria optimization in intensity modulated radiotherapy planning. In: Pardalos, PM.; Romeijn, HE., editors. Handbook of Optimization in Medicine. New York, NY, USA: Springer; 2009.
6. Spirou SV, Chui CS. A gradient inverse planning algorithm with dose-volume constraints. Med. Phys. 1998 Mar.25:321–333. [PubMed: 9547499]
7. Wu Q, Mohan R. Algorithms and functionality of an intensity modulated radiotherapy optimization system. Med. Phys. 2000 Apr.27:701–711. [PubMed: 10798692]
8. Miettinen, K. Nonlinear Multiobjective Optimization. Boston, MA, USA: Kluwer; 1999.
9. Marler R, Arora JS. Survey of multi-objective optimization methods for engineering. Struct. Multidisc. Optim. 2004; 26:293–297.
10. Bonnans, JF.; Shapiro, A. Perturbation analysis of optimization problems. New York, NY, USA: Springer-Verlag; 2000.
11. Jee KW, McShan DL, Fraass BA. Lexicographic ordering: Intuitive multicriteria optimization for IMRT. Phys. Med. Biol. 2007 Apr.52:1845–1861. [PubMed: 17374915]
12. Wilkens JJ, Alaly JR, Zakarian K, Thorstad WL, Deasy JO. IMRT treatment planning based on prioritizing prescription goals. Phys. Med. Biol. 2007 Mar.52:1675–1692. [PubMed: 17327656]
13. Clark VH, Chen Y, Wilkens J, Alaly JR, Zakaryan K, Deasy JO. IMRT treatment planning for prostate cancer using prioritized prescription optimization and mean-tail-dose functions. Linear Algebra Appl. 2008 Mar.428:1345–1364. [PubMed: 18974791]
14. Rosenthal R. Principles of multiobjective optimizaiton. Decis. Sci. 1985:133–152.
15. Rivera L, Yorke E, Kowalski A, Yang J, Radke RJ, Jackson A. Reduced-order constrained optimization (ROCO): Clinical application to head-and-neck IMRT. Med. Phys. 2013 Feb. 40:021715. [PubMed: 23387738]
16. Stabenau H, Rivera L, Yorke E, Yang J, Lu R, Radke RJ, Jackson A. Reduced order constrained optimization (ROCO): Clinical application to lung IMRT. Med. Phys. 2011 May.38:2731–2741. [PubMed: 21776810]
17. Lu R, Radke RJ, Happersett L, Yang J, Chui CS, Yorke E, Jackson A. Reduced-order parameter optimization for simplifying prostate IMRT planning. Phys. Med. Biol. 2007 Feb.52:849–870. [PubMed: 17228125]

18. Lu R, Radke RJ, Yang J, Happersett L, Yorke E, Jackson A. Reduced-order constrained optimization in IMRT planning. Phys. Med. Biol. 2008 Dec.53:6749–6766. [PubMed: 18997270]
19. Kalantzis, G.; Apte, A.; Radke, R.; Jackson, A. A reduced order memetic algorithm for constraint optimization in radiation therapy treatment planning; Proc. ACIS Int. Conf. Softw. Eng., Artif. Intell., Netw. Parallel /Distributed Comput; HI, USA. 2013. p. 225-230.
20. Mohan R, Chui C, Lidofsky L. Differential pencil beam dose computation model for photons. Med. Phys. 1986 Jan-Feb;13:64–73. [PubMed: 3951411]
21. Ahnesjo A, Saxner M, Trepp A. A pencil beam model for photon dose calculation. Med. Phys. 1992 Mar-Apr;19:263–273. [PubMed: 1584117]
22. Nocedal, J.; Wright, S. Numerical Optimization. 2nd ed.. New York, NY, USA: Springer Verlag; 2006.
23. Deasy JO, Blanco AI, Clark VH. CERR: A computational environment for radiotherapy research. Med. Phys. 2003 May.30:979–985. [PubMed: 12773007]
24. Deasy J, Lee E, Bortfeld T, Langer M, Zakarian K, Alaly J, Zhang Y, Liu H, Mohan R, Ahuja R, Pollack A, Purdy J, Rardin R. A collaboratory for radiation therapy treatment planning optimization research. Ann. Oper. Res. 2006; 148:55–63.
25. International Commission on Radiation Units. Bethesda, MD, USA: ICRU; 1993. ICRU International Commission on Radiation Units50 Prescribing, recording and reporting photon beam therapy. Report No. 50
26. Hristov D, Stavrev P, Sham E, Fallone BG. On the implementation of dose-volume objectives in gradient algorithms for inverse treatment planning. Med. Phys. 2002 May.29:848–856. [PubMed: 12033581]
27. Deasy JO. Multiple local minima in radiotherapy optimization problems with dose-volume constraints. Med. Phys. 1997 Jul.24:1157–1161. [PubMed: 9243478]
28. Deb, K. Multi-Objective Optimization Using Evolutionary Algorithms. Chichester, U.K.: Wiley; 2001.
29. Hoffmann H. Kernel PCA for novely detection. Pattern Recog. 2007; 40:863–874.
30. Romeihn HE, Ahuja RK, Dempsey JF. A new linear programming approach to radiation therapy treatment planning problems. Oper. Res. 2006; 54:201–216.
31. Men C, Gu X, Choi D, Majumdar A, Zheng Z, Mueller K, Jiang SB. GPU-based ultrafast IMRT plan optimization. Phys. Med. Biol. 2009 Nov.54:6565–6573. [PubMed: 19826201]
32. Theos F, Lagaris I, Papageorgiou D. PANMIN: sequential and parallel global optimization procedures with a variety of options for the local search strategy. Comput. Phys. Commun. 2004; 159:63–69.

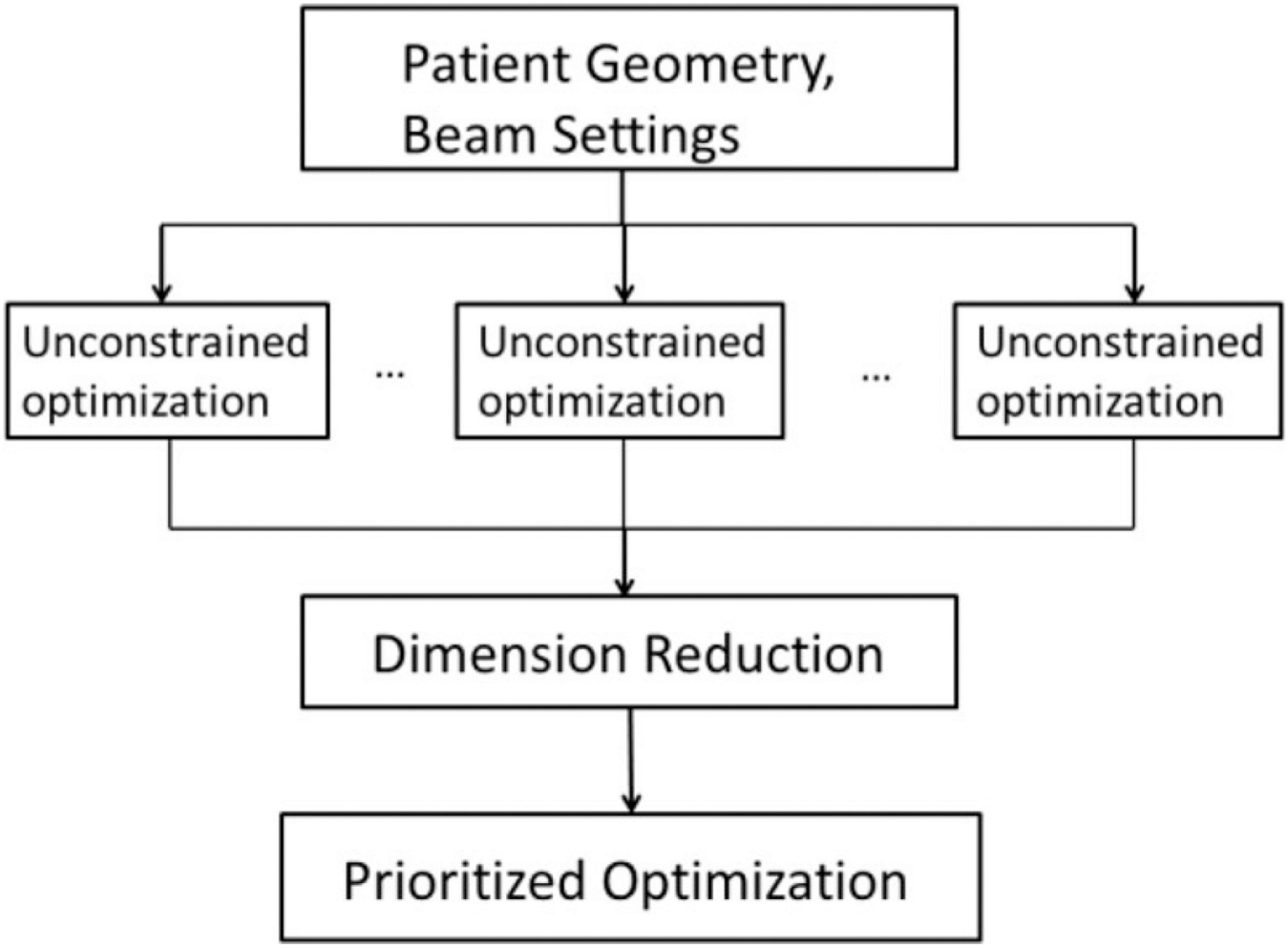

Fig. 1.
Generic outline of the reduced-order PO method.

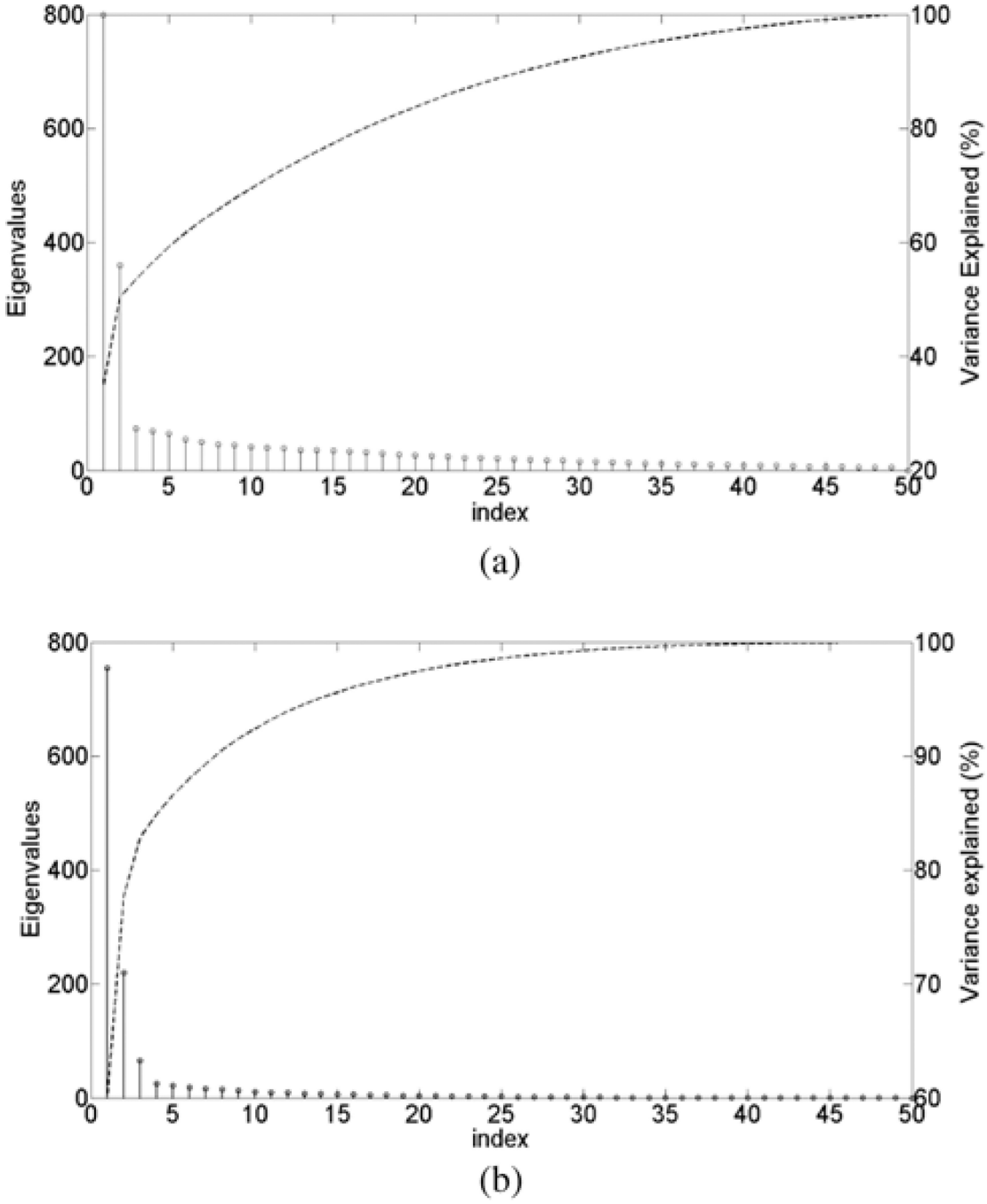

Fig. 2.

Screen plot of the first fifty eigenvalues obtained with the PCA of the unconstrained set of optimized plans (stem bars) for the prostate (a) and lung (b) case. The dashed line represents the percentage of variance explained as a function of the eigenvalues (left *y*-axis).

$$step\ 1: \min \frac{\sum_{j \in PTV} [D_{PTV}(y) - D_{presc}]^2}{V_{PTV}}$$

$$step\ 2: \min \frac{\sum_{j \in Rectum} D_j(y)}{V_{Rectum}}$$

$$step\ 3: \min \frac{\sum_{j \in Bladder} D_j(y)}{V_{Bladder}}$$

(a)

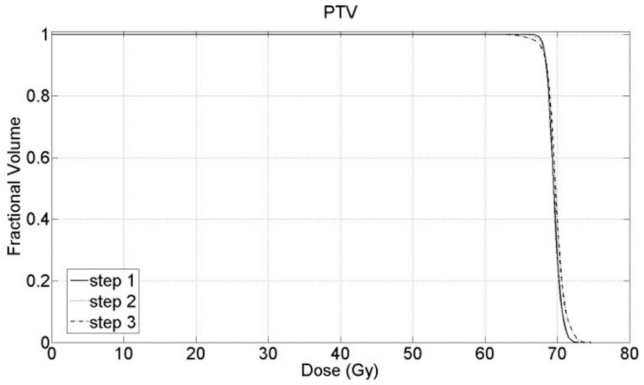

(b)

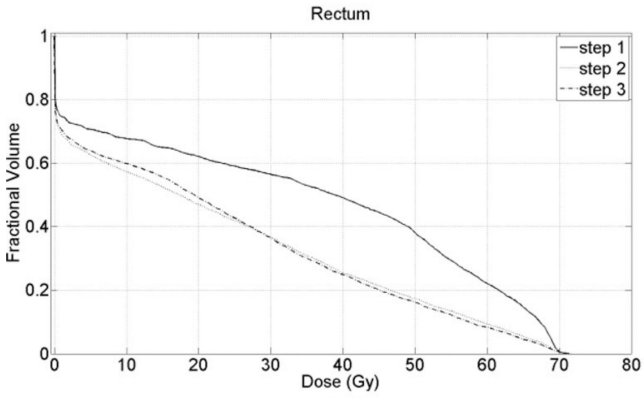

(c)

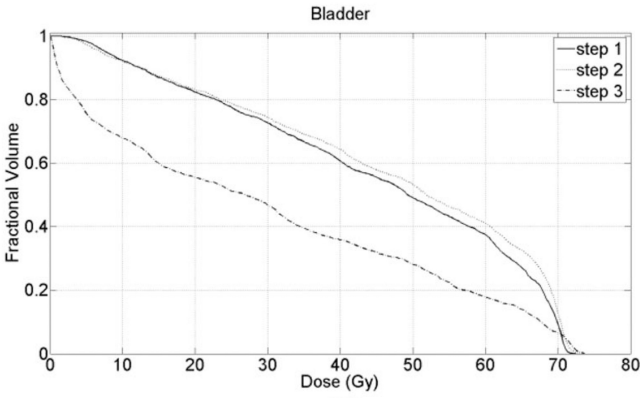

(d)

Fig. 3.

A simplified summary of the sequential optimization formulation (a), as used in this paper for the prostate case, and DVHs for each step of the reduced-order PO for the PTV (b), rectum (c), and bladder (d). A quadratic slip factor of 2.0 was used for the PTV in this set of optimizations.

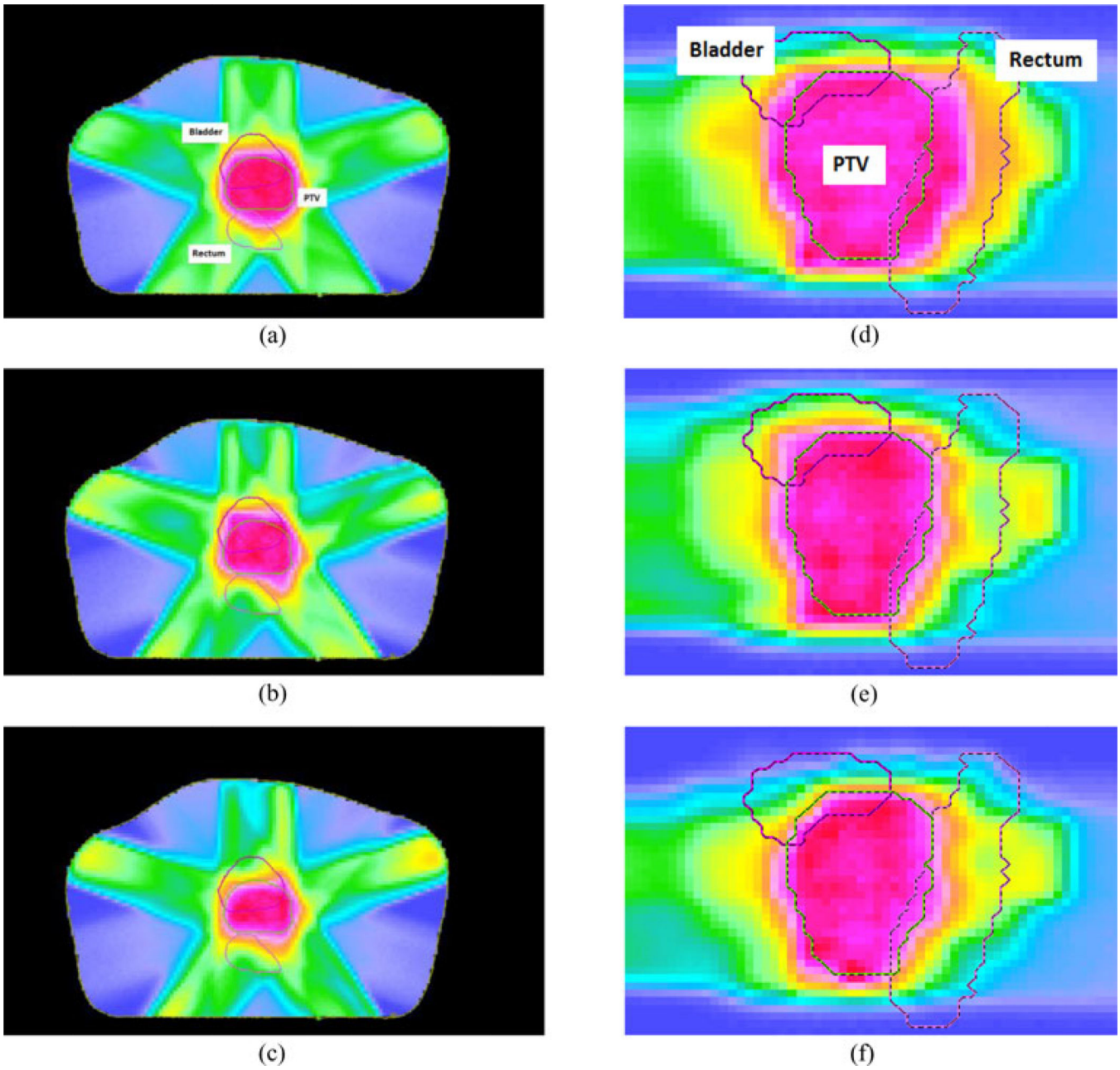

Fig. 4.

Traversal (left panel) and sagittal (right panel) view of the dose distribution for each step of the PO (Step 1: a, d; Step 2: b, e; Step 3: c, f). The outlined structures are (from top to bottom for traversal view; left to right for sagittal view) the bladder, PTV, and rectum.

$$step\ 1:\ min \frac{\sum_{j \in PTV} [D_{PTV}(y) - D_{presc}]^2}{V_{PTV}}$$

$$step\ 2:\ min \frac{\sum_{j \in Lung} D_j(y)}{V_{Lung}}$$

$$step\ 3:\ min \frac{\sum_{j \in Heart} D_j(y)}{V_{Heart}}$$

(a)

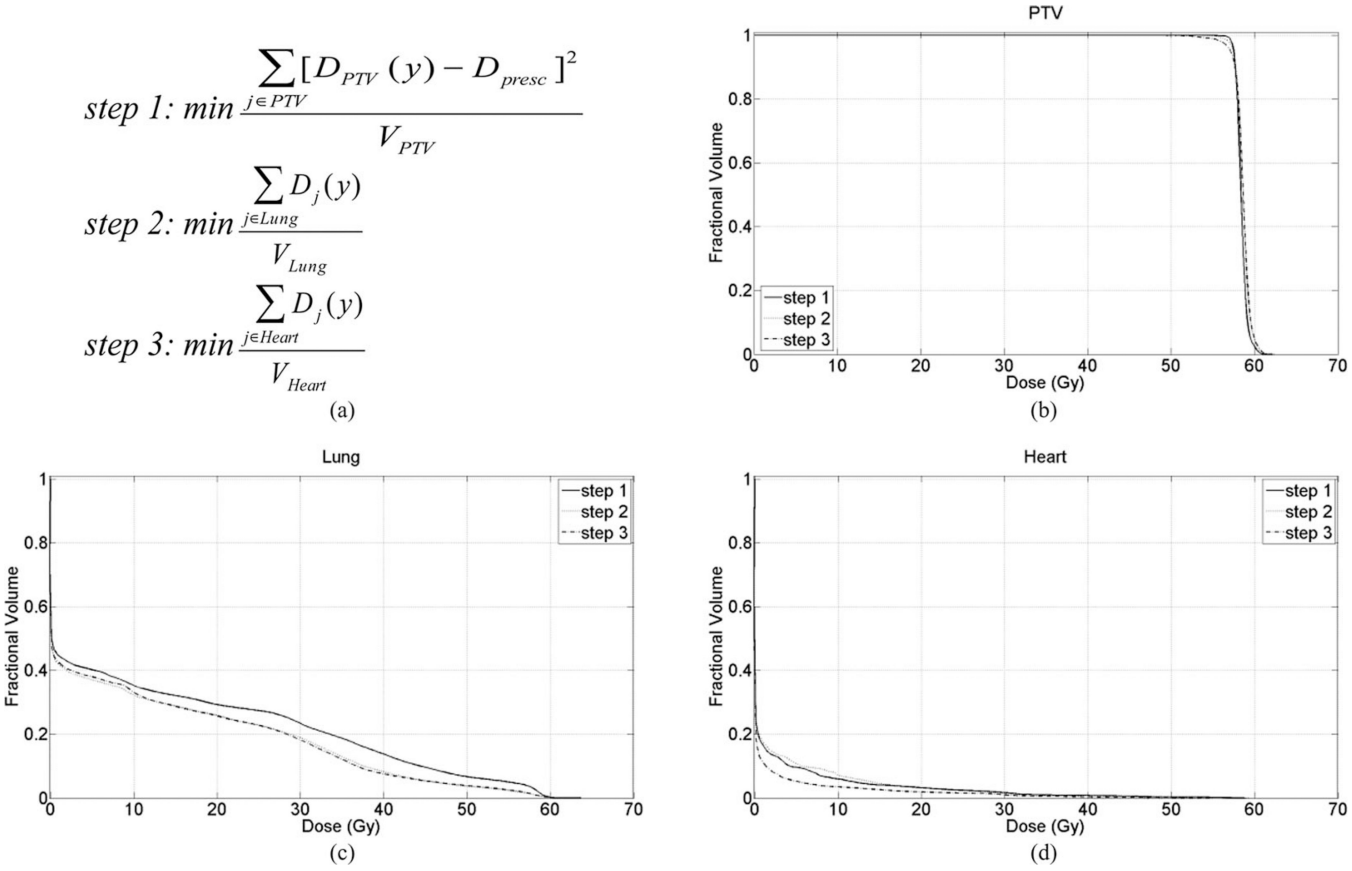

Fig. 5.

A simplified summary of the sequential optimization formulation (a), as used for the lung case in this paper, and the DVHs for each step of the reduced-order PO for the PTV (b), lung (c), and heart (d), structures respectively. A quadratic slip factor of 3 was used for the PTV in this set of optimizations.

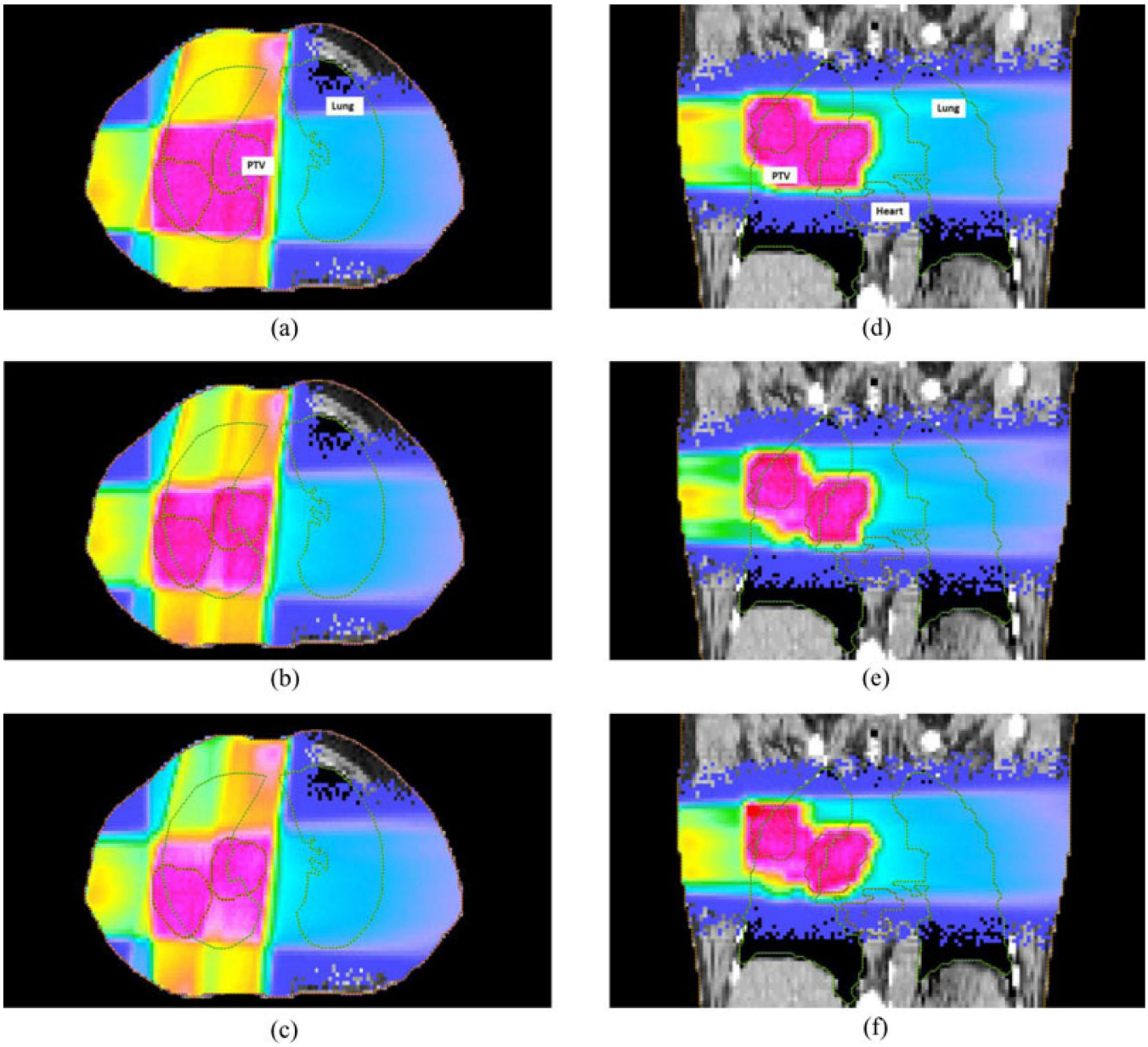

Fig. 6.

Traversal (left panel) and sagittal (right panel) view of the dose distribution for each step of the PO (Step 1: a, d; Step 2: b, e; Step 3: c, f). The outlined structures are the lungs, PTV, and heart.

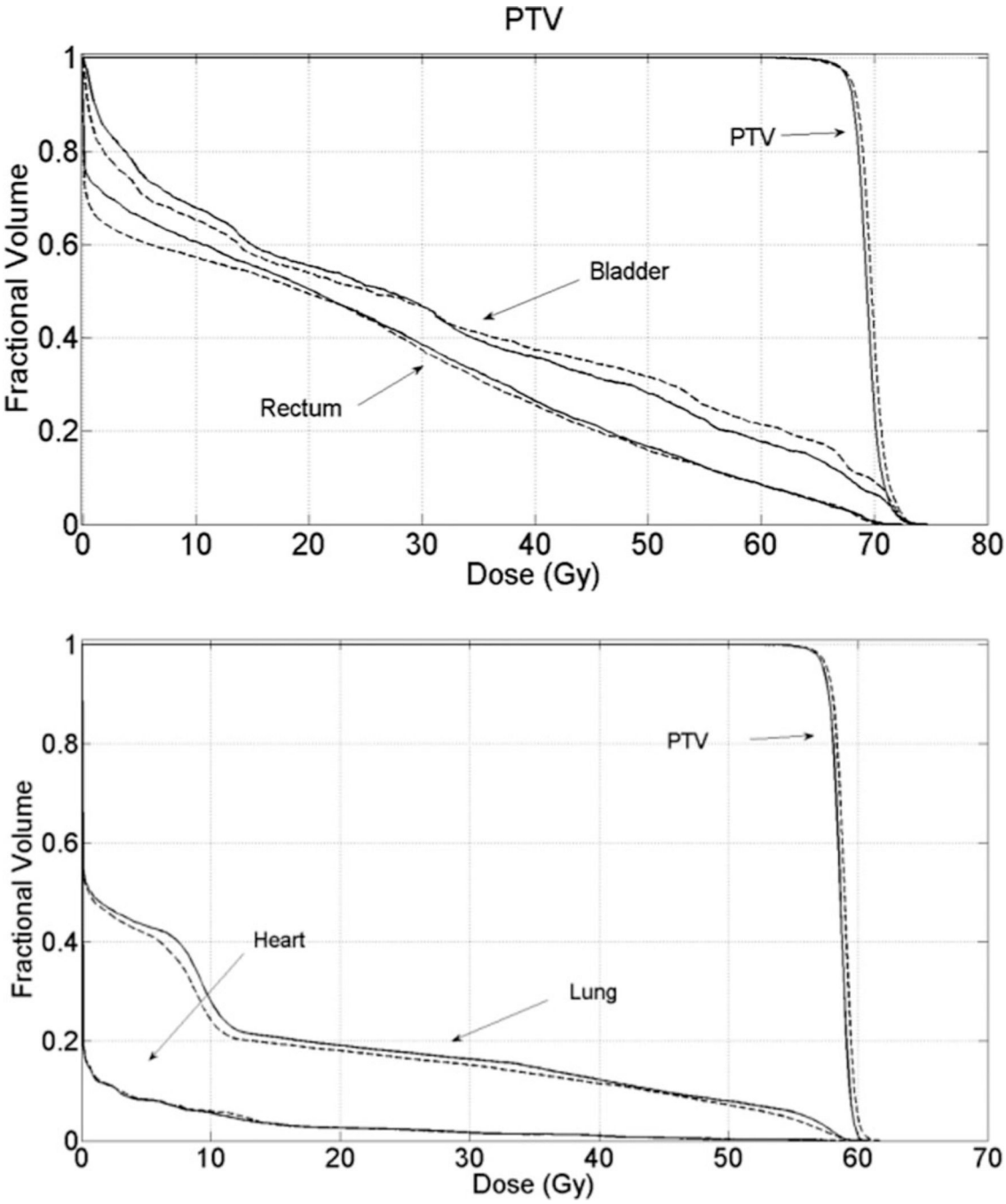

Fig. 7.
DVHs of the PO with (solid line) and without (dashed line) dimensionality reduction for the two cases.

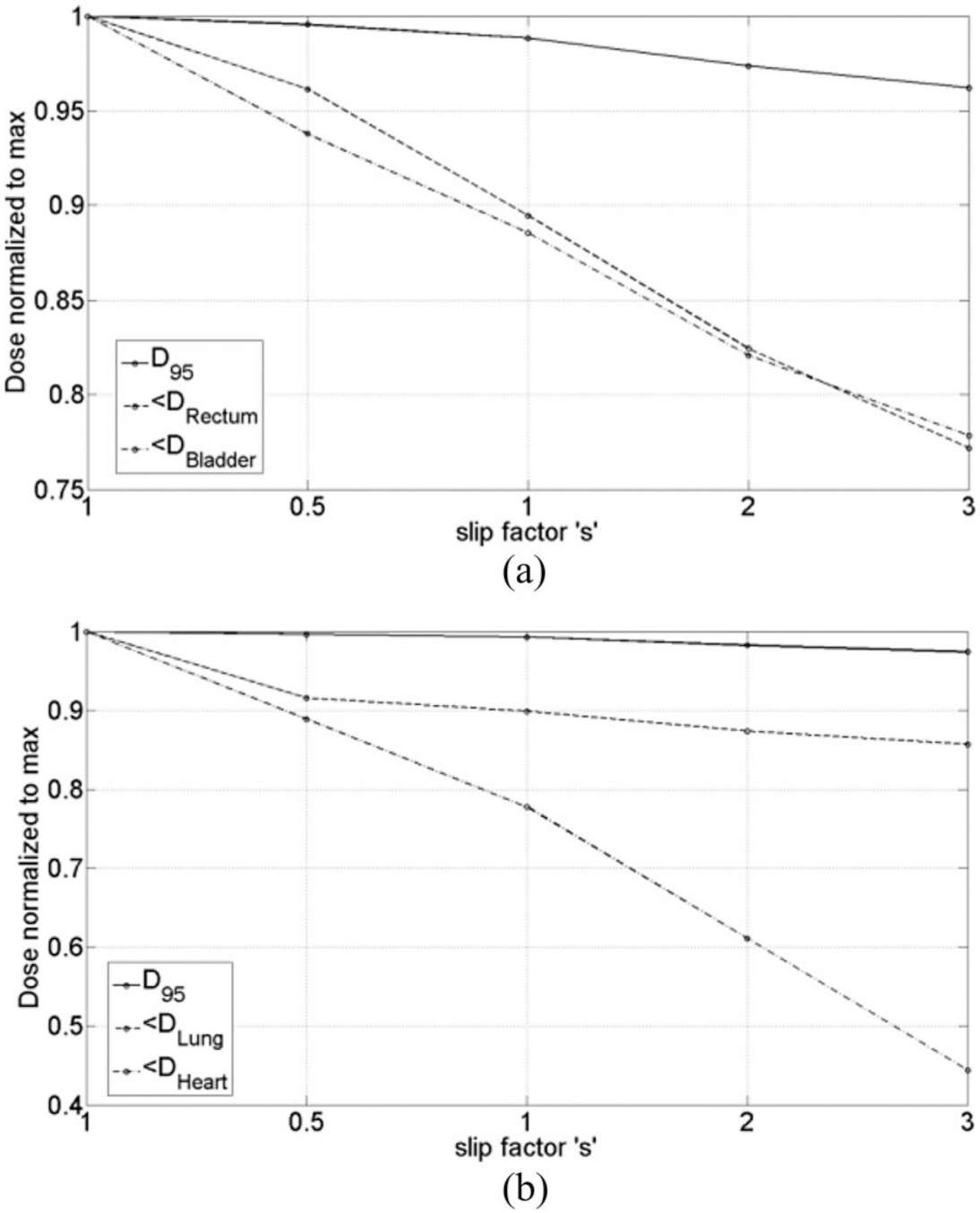

Fig. 8.
Effect of the slip factor s on the reduced-order PO for the prostate and lung case.

TABLE I

Summary Metrics for the PTV and Two OARs at Each Step of the Prioritized Optimization Algorithm Using a Slip Factor of 2

Metric	Step 1	Step 2	Step 3
PTV			
D_{95}	68.4	67.9	67.0
s.t.d.	0.59	0.83	1.17
$\langle D \rangle$	69.7	69.6	69.8
Rectum			
D_{min}	0.1	0.1	0.1
D_{max}	71.7	70.9	71.7
$\langle D \rangle$	32.3	26.8	26.8
Bladder			
D_{min}	1.7	1.5	0.1
D_{max}	72.5	73.1	72.7
$\langle D \rangle$	45.5	46.2	37.2

Dose values are in Gy.

TABLE II

Dosimetric Evaluation Parameters for the PTV and Two OARs at Each Step of the Optimization Algorithm

Metric	Step 1	Step 2	Step 3
PTV			
D_{95}	59.0	58.3	57.6
s.t.d.	0.48	0.72	1.21
$\langle D \rangle$	58.1	57.4	56.5
Lung			
D_{min}	0.1	0.1	0.1
D_{max}	61.7	60.9	60.7
$\langle D \rangle$	11.9	10.2	10.2
Heart			
D_{min}	1.7	1.5	0.1
D_{max}	59.1	59.3	48.9
$\langle D \rangle$	1.8	1.8	0.8

Dose values are in Gy, and a slip factor of 3 was used.

TABLE III

Speedup Factors for Each Step of the Prioritized Optimization for the Prostate and Lung Case

Plan	Step 1	Step 2	Step 3
Prostate			
	36.8	37.8	34.3
Lung			
	49.9	46.5	44.1